

Article

Naphthoquinone Derivatives with Anti-Inflammatory Activity from Mangrove-Derived Endophytic Fungus *Talaromyces* sp. SK-S009

Hongju Liu ^{1,*}, Chong Yan ¹, Changqun Li ¹, Tingting You ¹ and Zhigang She ^{2,*} 

¹ School of Pharmacy, Guangdong Medical University, 523808 Dongguan, China; jdsbj2000@163.com (C.Y.); lqcstary@163.com (C.L.); youtt2013@163.com (T.Y.)

² School of Chemistry, Sun Yat-Sen University, 510275 Guangzhou, China

* Correspondence: liuhj8@mail2.sysu.edu.cn (H.L.); ceshzhg@mail.sysu.edu.cn (Z.S.); Tel./Fax: +86-20-84113356 (Z.S.)

Received: 5 December 2019; Accepted: 22 January 2020; Published: 29 January 2020



Abstract: Twelve 1, 4-naphthoquinone derivatives, including two new (**1** and **2**) and 10 known (**3–12**), were obtained from endophytic fungus *Talaromyces* sp. SK-S009 isolated from the fruit of *Kandelia obovata*. All structures were identified through extensive analysis of the nuclear magnetic resonance (NMR), mass spectrometry (MS) and circular dichroism (CD), as well as by comparison with literature data. These compounds significantly inhibited the lipopolysaccharide (LPS)-induced nitric oxide (NO) production in the murine macrophage cell line (RAW 264.7 cells). The half maximal inhibitory concentration (IC₅₀) values, except for compound **2**, were lower than that of indomethacin (26.3 μM). Compound **9** inhibited the LPS-induced inducible nitric oxide synthase (iNOS) and cyclooxygenase-2 (COX-2) mRNA expressions in RAW 264.7 macrophages. Additionally, compound **9** reduced the mRNA levels of pro-inflammatory factors interleukin (IL)1β, IL-6, and tumor necrosis factor (TNF)-α. The results of this study demonstrated that these 1, 4-naphthoquinone derivatives can inhibit LPS-induced inflammation.

Keywords: 1,4-naphthoquinones; *Talaromyces* sp.; marine fungus; anti-inflammatory

1. Introduction

Inflammation is a normal immune process and one of the most important ways to protect the body from infection and tissue injury. However, prolonged or excessive inflammation can lead to a variety of diseases. Many diseases, such as arthritis, inflammatory bowel disease, neurodegenerative disorders, and septic shock syndrome, are related to inflammation. During the inflammatory process, the immune monocytes and macrophages can be stimulated and overexpress pro-inflammatory cytokines, including tumor necrosis factor (TNF)-α, interleukin (IL)-1β, and IL-6, as well as inflammatory factors such as nitric oxide (NO) and prostaglandin E2 (PGE2), produced by inducible nitric oxide synthase (iNOS) and cyclooxygenase-2 (COX-2), respectively [1]. Overproduction of these factors can lead to cell damage and inflammatory disease [2]. Therefore, inhibition of the production of these inflammatory mediators is an effective way to treat the inflammatory diseases [3].

Marine-derived endophytic fungi are important sources of bioactive compounds [4–7]. During our investigation of mangrove-derived endophytic fungus as sources of bioactive secondary metabolites, we isolated the endophytic fungus *Talaromyces* sp. SK-S009 from the fruit of *Kandelia obovata*. Organic extracts of rice solid culture showed significant anti-inflammatory activity. Chemical investigation of the extracts led to the isolation of twelve 1, 4-naphthoquinone derivatives (Figure 1). Here, we report the isolation, structure determination, and anti-inflammatory activities of 1, 4-naphthoquinone derivatives (**1–12**).

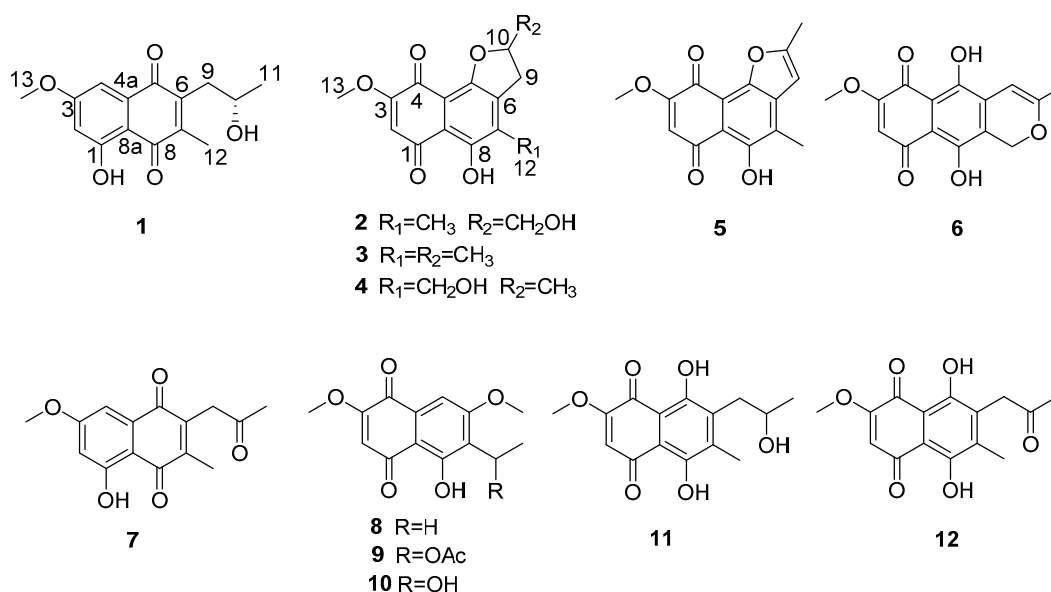


Figure 1. Structures of compounds 1–12.

2. Results and Discussion

2.1. Metabolites Isolation

The EtOAc extract of the fermentation was fractionated by repeated silica gel chromatography and Sephadex LH-20 column chromatography, as well as reversed phase high-performance liquid chromatography (RP-HPLC) to yield twelve 1,4-naphthoquinone derivatives, including two new (**1** and **2**) and 10 known (**3**–**12**). The structures of the known compounds were identified as anhydrojavanicin (**3**) [8], 2,3-dihydro-5-hydroxy-4-hydroxymethyl-8-methoxy-2-methylnaphtho[1,2-b]furan-6,9-dione (**4**) [9], anhydrojavanicin (**5**) [10], anhydrofusarubin (**6**) [11], 2-acetyl-3-methyl-5-hydroxy-7-methoxynaphthazarin (**7**) [12], 6-ethyl-2,7-dimethoxyjuglone (**8**) [13,14], 6-[1-(acetyloxy)ethyl]-5-hydroxy-2,7-dimethoxy-1,4-naphthalenedione (**9**) [15], 5-hydroxy-6-(1-hydroxyethyl)-2,7-dimethoxy-1,4-naphthalenedione (**10**) [16], solaniol (**11**) [17], and javanicin (**12**) [18], by comparison of their spectroscopic data with those reported in the literature.

2.2. Structure Identification

Talanaphthoquinone A (**1**) was isolated as a yellow, amorphous powder. The high-resolution electrospray ionization mass spectrometry (HRESIMS) spectrum (see Supplementary Materials Figure S1) displayed a molecular ion peak at m/z 275.09223 $[M - H]^-$ (calcd. for 275.09195), implying the molecular formula C₁₅H₁₅O₅ (eight degrees of unsaturation). The ¹H NMR spectrum (Table 1) showed signals for one phenolic hydroxyl proton δ_H 12.38 (s, HO-1), two meta-coupled aromatic protons (δ_H 7.17 (d, J = 2.5 Hz, H-4), δ_H 6.63 (d, J = 2.5 Hz, H-2)), two methyl groups (δ_H 2.21 (s, H₃-12), δ_H 1.31 (d, J = 6.2 Hz, H₃-11)), one methoxy (δ_H 3.90 (s, OCH₃-13)), one oxygenated methine (δ_H 4.04 (dd, J = 11.9, 6.0 Hz, OCH-10)), and one methylene (δ_H 2.81 (s, H_a-9), δ_H 2.80 (d, J = 1.7 Hz, H_b-9)). The ¹³C NMR data (Table 1) revealed two carbonyls (δ_C 188.6, 185.2), eight sp²-hybridized olefinic or aromatic carbons (δ_C 165.9, 164.2, 145.7, 144.6, 133.7, 109.7, 107.8, 106.1), three methyl groups (δ_C 56.1, 12.9, 24.4), one methylene (δ_C 36.8), and one methine (δ_C 67.9). The planar structure of **1** was mainly established by HMBC and COSY correlations (Figure 2). The HMBC correlations from one aromatic proton H-2 (δ_H 6.63) to sp² carbons C-3 (δ_C 165.9) and C-8a (δ_C 109.7), H-4 (δ_H 7.17) to C-2 (δ_C 106.1), C-3, C-5 (δ_C 185.2) and C-8a, led to the identification of the presence of a 1,3,4,5-tetrasubstituted benzene ring with a hydroxy, a methoxy, and two carbonyl groups attached at the C-1, C-3, C-4a, and C-8a, respectively. A methoxy group (δ_H 3.90, δ_C 56.1) was located at C-3, supported by its HMBC

correlations with C-3. The HMBC correlations of the hydroxyl proton at δ_H 12.38 with C-2 and C-8a confirmed an angular 1, 4-naphthaquinone structure having an intra-molecularly hydrogen-bonded hydroxyl group at C-1. The COSY correlations of H-10 with H₂-9 and H₃-11, combined with the chemical shift of C-10 (δ_C 67.9), showed the presence of one 2-hydroxypropyl group. The HMBC correlations from H-12 to C-6 (δ_C 144.6), C-7 (δ_C 145.7), and C-8 (δ_C 188.6), H-9 to C-5, C-6, and C-7 revealed the presence of another ring 1, 4-quinone, 2-hydroxypropyl group and CH₃-12 were attached to the C-6 and C-7 of the naphthaquinone ring, respectively. Mosher's method was tried to identify the absolute configuration of C-10 [19]. Unfortunately, alpha-methoxy-alpha-trifluoromethylphenylacetic acid (MTPA) esters were not detected. As a result, the absolute configuration of C-10 was determined by comparing experimental and calculated electronic circular dichroism (ECD) spectra [20]. As shown in Figure 3, the calculated ECD curves of 10S was basically consistent with the CD curves obtained experimentally. Therefore, compound **1** was identified as shown in Figure 1.

Table 1. The ¹H and ¹³C NMR data (CDCl₃, 500/125 MHz) of compounds **1** and **2**.

Position	1		2	
	δ_C	δ_H (J in Hz)	δ_C	δ_H (J in Hz)
1	164.2, C	-	190.1, C	-
2	106.1, C	6.63, d (2.5)	109.2, CH	6.07, s
3	165.9, C	-	161.4, C	-
4	107.8, C	7.17, d (2.5)	177.6, C	-
4a	133.7, C	-	109.1, C	-
5	185.2, C	-	155.0, C	-
6	144.6, C	-	139.0, C	-
7	145.7, C	-	134.2, C	-
8	188.6, C	-	157.3, C	-
8a	109.7, C	-	110.3, C	-
9	36.8, CH ₂	2.81, s 2.80, d (1.7)	29.9, CH ₂	3.04, dd (7.1,16.6); 3.20, dd (9.4,17.0)
10	67.9, CH	4.04, dd (11.9, 6.0)	86.2, CH	5.15, m
11	24.4, CH ₃	1.31, d (6.2)	64.5, CH ₂	3.76, d (8.6); 4.02, d (12.7)
12	12.9, CH ₃	2.21, s	13.3, CH ₃	2.25, s
13	56.1, CH ₃	3.9, s	56.7, CH ₃	3.88, s
1-OH	-	12.38, s	-	13.47, s

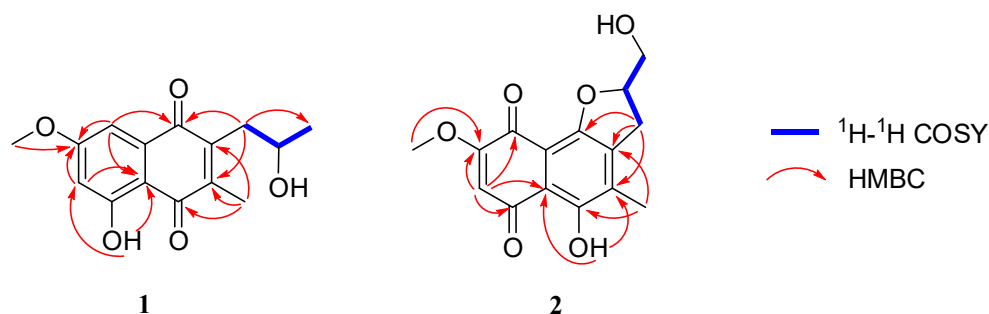


Figure 2. Key HMBC (red arrows) and COSY (blue bold lines) correlations of compounds **1** and **2**.

Talanaphthoquinone B (**2**) was isolated as a red solid with $[\alpha]_D^{25}$: -16.8 (*c* 0.1, MeOH). The HRESIMS spectrum displayed a negative ion peak at m/z 307.08218 $[M+H_2O-H]^-$ (calcd. for C₁₅H₁₅O₇, 307.08178), corresponding to the molecular formula C₁₅H₁₄O₆, implying nine degrees of unsaturation. The UV and IR spectra of **2** were similar to those of talanaphthoquinone A, indicating that they were structurally related. Aside from the characteristic naphthoquinone NMR signals due to two quinone carbonyls (δ_C 190.1, 177.6) and eight aromatic/olefinic carbon resonances (δ_C 161.4, 157.3, 155.0, 139.0, 134.2, 110.3, 109.3, 109.1), ¹H- and ¹³C-NMR spectrum (Table 1) showed the presence of

signals due to two methyl groups (δ_{H} 3.88, δ_{C} 56.7, OCH₃-13; δ_{H} 2.25, δ_{C} 13.3, CH₃-12), two methylene groups (δ_{H} 3.20 (dd, $J = 17.0, 9.3$ Hz, 1H), δ_{H} 3.04 (dd, $J = 16.6, 7.0$ Hz, 1H), δ_{C} 29.9, CH₂-9; δ_{H} 4.02 (d, $J = 12.7$ Hz, 1H), δ_{H} 3.76 (d, $J = 8.7$ Hz, 1H), δ_{C} 64.5, OCH₂-11], an oxymethine group (δ_{H} 5.15 (d, $J = 3.7$ Hz), δ_{C} 86.2, OCH-10), one phenolic hydroxyl proton (δ_{H} 13.47 (s), HO-8), and one aromatic proton (δ_{H} 6.07 (s), H-2). The COSY correlations (Figure 2) of H-10 with H₂-9 and H₂-11 showed the presence of an independent spin coupling system -CH₂-CH-CH₂. The chemical shift of C-11 indicated one hydroxyl group was located on C-11. HMBC spectrum (Figure 2) showed that H-2 was correlated with C-1 (δ_{C} 190.1), C-3 (δ_{C} 161.4), C-4 (δ_{C} 177.6), and C-8a (δ_{C} 110.3), which could confirm that the only aromatic hydrogen was attached to the C-2 (δ_{C} 109.2). A methoxyl group was linked to olefinic carbon C-3, supported by the HMBC correlation of H-13 with C-3. The HMBC correlation of H-12 with C-6 (δ_{C} 139.0), C-7 (δ_{C} 134.2), and C-8 (δ_{C} 157.3) indicated that the methyl group was connected to the C-7. The HMBC correlation of H-9 with C-5 (δ_{C} 155.0), C-6, C-7, indicated that C-9 was attached to the C-6. Phenolic hydroxyl group was located at C-8, as indicated by the HMBC correlation with C-7 and C-8. The naphthoquinone structure unit explained seven of the eight degrees of unsaturation in **2**, implied by the molecular formula. The remaining one degree of unsaturation, together with downfield chemical shift of C-10 (δ_{C} 86.2), indicated that C-10 was attached to C-5 to fuse a furan ring. In the light of the chemical shift of C-11 (δ_{C} 64.5), the C-11 was a hydroxymethyl group. Therefore, the planar structure of compound **2** was elucidated as shown in Figure 1.

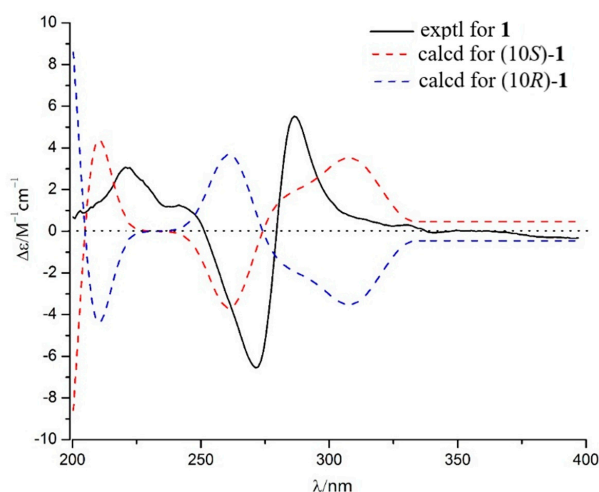


Figure 3. Calculated and experimental electronic circular dichroism (ECD) spectra of **1**.

2.3. Inhibitory Effects on NO Production

All these isolates were tested for their inhibitory activities against lipopolysaccharide (LPS)-activated NO production in the murine macrophage cell line (RAW 264.7 cells). As shown in Table 2, all compounds could inhibit the production of NO with IC₅₀ values ranging from 1.7 to 49.7 μM , while IC₅₀ of indomethacin was 26.3 μM . It is suggested that the 1, 4-naphthoquinone is the active center of anti-inflammatory effect. Compound **2** has only one more hydroxyl group at position 11 than compound **3** in structure, but the inhibitory activity was apparently weaker, which indicates that the hydroxyl group at position 11 was not conducive to the anti-inflammatory activity. Their cytotoxic effects on RAW 264.7 cell lines was evaluated by the MTT assay. Six compounds (**2–6** and **8**) showed no cytotoxicity at a concentration of 50 μM . Six compounds (**1, 7, 9, 10, 11** and **12**) revealed some cytotoxicity with the selective index ($\text{SI} = \text{CC}_{50}/\text{IC}_{50}$) values from 2.1 to 29.6 (Table 2). The cytotoxicity data indicated that the third ring on the naphthoquinone can reduce the cytotoxicity to macrophage of mice. Compound **9** had lower cytotoxicity than **10**, which revealed that the hydroxyacetylation on the side chain can also reduce the cytotoxicity.

Table 2. Inhibitory activity of all compounds 1–12 against lipopolysaccharide (LPS)-induced NO production in the murine macrophage cell line (RAW 264.7 cells).

Compounds	IC ₅₀ (μM)	CC ₅₀ (μM) ^a	SI ^b
1	3.9 ± 0.5	30.7 ± 0.5	7.9
2	49.7 ± 1.5	-	
3	16.0 ± 0.2	-	
4	22.6 ± 0.5	-	
5	11.2 ± 0.3	-	
6	5.2 ± 0.1	-	
7	14.4 ± 0.6	51.4 ± 1.5	3.6
8	7.7 ± 0.3	-	
9	1.7 ± 0.2	50.3 ± 1.5	29.6
10	7.5 ± 0.2	15.8 ± 0.4	2.1
11	15.5 ± 0.6	59.2 ± 1.5	3.8
12	5.6 ± 0.3	48.4 ± 1.3	8.6
Indomethacin ^c	26.3 ± 0.6		

^a Values are taken as the means ± standard deviation, $n = 3$; ^b SI, selectivity index, calculated by CC_{50}/IC_{50} ; ^c Positive control; - No cytotoxicity was observed at a concentration of 50 μM.

2.4. Inhibitory Effects on the Production of Inducible Nitric Oxide Synthase (iNOS), Cyclooxygenase-2 (COX-2), and Pro-Inflammatory Factors

Based on the results of inhibitory effects on NO production, compound 9 was found to be a significant inhibitor of NO with low cytotoxicity (SI = 29.6). We have further investigated the effects of CC₅₀/IC₅₀ on mRNA expressions of inducible nitric oxide synthase (iNOS), cyclooxygenase-2 (COX-2), and the pro-inflammatory cytokines tumor necrosis factor (TNF)-α, interleukin (IL)-1β, and IL-6 in LPS-stimulated RAW 264.7 cells using real-time polymerase chain reaction (RT-PCR) analysis. As shown in Figure 4A–E, compound 9 apparently reduced the mRNA expressions of iNOS, COX-2, TNF-α, IL-1β, and IL-6 in a dose-dependent manner. Especially at the concentration of 2.0 μM, compound 9 inhibited the mRNA expressions of TNF-α, IL-1β, and IL-6 by about 80% compared with the control groups.

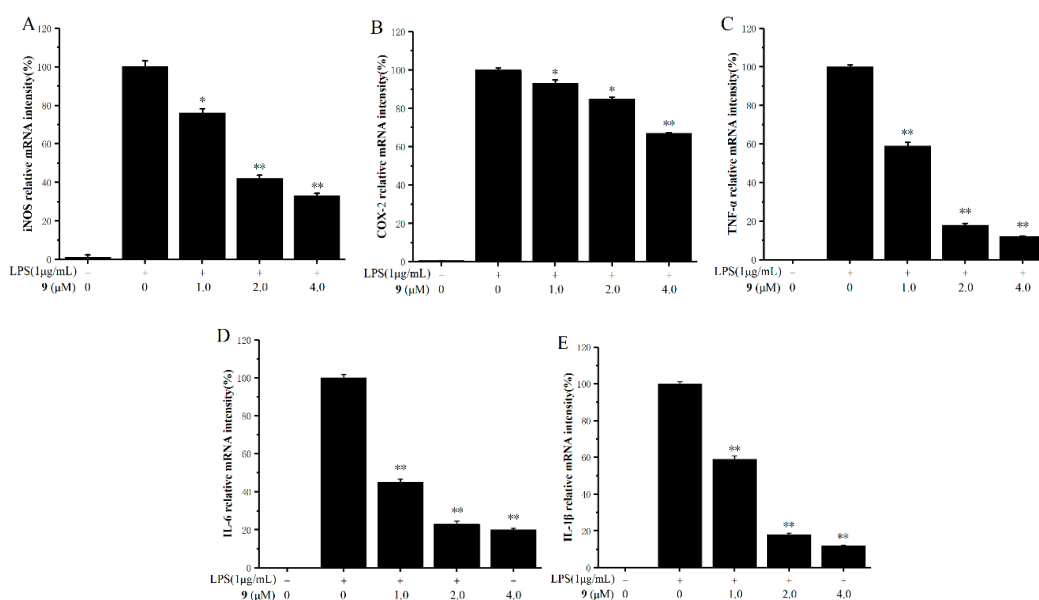


Figure 4. RAW 264.7 murine macrophage cells were pre-incubated for 12h, and then cells were pretreated with compound 9 at the indicated concentration for 1 h and incubated with LPS (1 μg/mL) for 12h (real-time PCR). The effect of compound 9 on the mRNA expressions of inducible nitric oxide synthase (iNOS) (A), cyclooxygenase-2 (COX-2)(B), tumor necrosis factor (TNF)-α (C), interleukin (IL)-6 (D), and IL-1β (E) were detected by real-time PCR. The data represent the mean values ± SD of three experiments, * $p < 0.05$, ** $p < 0.01$ compared to LPS-treated group.

3. Materials and Methods

3.1. General Experimental Procedures

The 1D and 2D NMR data were recorded on Bruker Avance 400 and 500 spectrometer (Bruker BioSpin Corporation, Billerica, MA, USA), in which all chemical shifts (δ) are given in ppm with reference to tetramethylsilane (TMS), and coupling constants (J) are given in Hz. EIMS data were measured on a dual stage quadrupole electron impact (DSQ EI)-mass spectrometer (Thermo, Shanghai, China) and the high-resolution electrospray ionization mass spectrometry (HRESIMS) were determined with a quadrupole time of flight (Q-TOF) high-resolution mass spectrometer (Waters Corporation, Synapt G2-Si, Milford, MA, USA). UV data were measured on a UV-240 spectrophotometer (Shimadzu, Beijing, China). IR data were recorded on a Nicolet 5DX-FTIR (Thermo Fisher Scientific, Inc., Hudson, NH), in KBr discs. Melting points were measured on an X-4 micromelting-point apparatus (Cany Precision Instruments Co., Ltd., Shanghai, China, uncorrected). Column chromatography (CC) was carried out on silica gel (200–300 mesh, Qingdao Marine Chemical Factory, Qingdao, China) and Sephadex LH-20 (Amersham Pharmacia, Piscataway, NJ, USA). GF-254 precoated silica gel plates (Qingdao Huang Hai Chemical Group Co., Qingdao, China) were used for thin layer chromatography. Semipreparative HPLC separation was performed on a Hitachi Primaide 1430 HPLC system (HITACHI, Tokyo, Japan) using a C₁₈ column (Phenomenex, Torrance, CA, USA; 250 × 10 mm, 5 μ m) with the flow rate of 2.0 mL/min.

3.2. Fungal Material

The fungal strain used in this study was isolated from the fresh fruit of *Kandelia obovata*, which was collected from Shankou National Mangrove Nature Reserve in the South China Sea in September 2013. It was separated and identified by Senhua Chen using the standard protocol [21]. The sequence data obtained from the fungal strain were deposited at Gen Bank with accession no. MK368459. A BLAST search result revealed that the sequence was the most similar (100%) to the sequence of *Talaromyces amestolkiae* (KT445914.1). A voucher strain was deposited in School of Chemistry, Sun Yat-Sen University, Guangzhou, China.

3.3. Extraction and Isolation

The fungus *Talaromyces* sp. SK-S009 was fermented on autoclaved rice solid-substrate medium in 80 500-mL Erlenmeyer flasks (each containing 50 g rice and 50 mL water with 3‰ of saline) for 28 days at 25 °C. Following incubation, the mycelia and solid rice medium were extracted with EtOAc. The organic solvent was filtered and concentrated under reduced pressure to yield 40 g organic extract. The extract was subjected to silica gel CC using gradient elution with petroleum ether-EtOAc from 90:10 to 0:100 (v/v) to give 14 fractions (fractions 1–14). Fraction 3 (600 mg) was applied to Sephadex LH-20 CC and eluted with CHCl₃/MeOH (1:1) to obtain seven subfractions (fractions 3.1–3.7). Fraction 3.4 (100 mg) was further purified by RP-HPLC (70% MeOH in H₂O) to afford **5** (12.1 mg, t_R = 10.0 min) and **1** (3.6 mg, t_R = 15.6 min). Fraction 3.7 (41 mg) was further purified by RP-HPLC (65% MeOH in H₂O) to afford **7** (5.8 mg, t_R = 22.0 min). Fraction 5 (560 mg) was further purified by RP-HPLC (70% MeOH in H₂O) to afford **12** (10.8 mg, t_R = 15.2 min), **3** (15.4 mg, t_R = 18.6 min), and **11** (8.6 mg, t_R = 26.1 min). Fraction 7 (503 mg) was further purified by silica gel CC using 80% EtOAc-light petroleum to afford seven subfractions (fractions 7.1–7.7). Fraction 7.3 (90 mg) was further purified by RP-HPLC (60% MeOH in H₂O) to afford **4** (20 mg, t_R = 14.5 min). Fraction 8 (870 mg) was applied to Sephadex LH-20 CC, eluted with CHCl₃/MeOH (1:1), to obtain 10 subfractions (fractions 8.1–8.10). Fraction 8.5 (25 mg) was further purified by Sephadex LH-20 CC, eluted with CHCl₃/MeOH (1:1), to afford **2** (3.3 mg). Fraction 8.7 (40 mg) was further purified by Sephadex LH-20 CC, eluted with CHCl₃/MeOH (1:1), to afford **6** (13.3 mg). Fraction 9 (680 mg) was applied to silica gel CC using 60% EtOAc-petroleum ether to afford seven subfractions (fractions 9.1–9.7). Fraction 10.3 was further

purified by RP-HPLC (50% MeOH in H₂O) to afford **8** (7.3 mg, t_R = 12.5 min), **9** (9.1 mg, t_R = 18.1 min), and **10** (20 mg, t_R = 20.4 min).

3.3.1. Talanaphthoquinone A (**1**)

Yellow powder [α]_D²⁵: −17.0 (c 0.1, MeOH); IR (KBr) ν_{\max} : 3375, 1655, 1633, 1602, 1576, 1379, 1302, 1207, 1167, 1113, 954, 817, 773 cm^{−1}. UV (MeOH) λ_{\max} (log ϵ): 268 (2.34), 219 (3.63) nm. The ¹H and ¹³C NMR spectroscopic data, see Table 1; HRESIMS (m/z 275.09223 [M − H][−], calcd. for C₁₅H₁₅O₅, 275.09195).

3.3.2. Talanaphthoquinone B (**2**)

Red solid [α]_D²⁵: −16.8 (c 0.1, MeOH); m.p. 157.7–159.3 °C; IR (KBr) ν_{\max} : 3422, 2981, 1672, 1636, 1587, 1473, 1452, 1252, 1221, 1165, 1091, 1031, 962, 930, 886, 863, 816, 790 cm^{−1}. UV (MeOH) λ_{\max} (log ϵ): 300 (2.45), 225 (3.89) nm. The ¹H and ¹³C NMR spectroscopic data, see Table 1; HRESIMS (m/z 307.08218 [M+H₂O-H][−], calcd. for C₁₅H₁₅O₇, 307.08178).

3.4. Measurement of NO Production and Cell Viability

The nitrite/nitrate oxidized from NO was detected by the Griess reagent as previously reported with slight modifications [22,23]. The murine macrophage cell line (RAW 264.7 cells) were seeded in 96-well plates at a density of 1 × 10⁵ cells/well and preincubated for 12 h. The tested compounds were dissolved in dimethylsulfoxide (DMSO) and diluted with Dulbecco's Modified Eagle Medium (DMEM) medium to a final concentration (final DMSO concentration <0.1% in all assays). Indomethacin was used as the positive control. Cells were stimulated with 1 µg/mL of lipopolysaccharide (LPS, Sigma, St. Louis, MO, USA) with or without tested compounds for 24 h. Then culture supernatant was mixed with an equal volume of Griess reagent I and II (Beyotime, Shanghai, China), and measured at 540 nm using a microplate reader (Bio-Rad Laboratories, Inc., Kyoto, Japan). Cell viability was evaluated using MTT assay [24].

3.5. Real-Time PCR

RAW264.7 cells were placed in a 6-well plate at a density of 1 × 10⁶ cells/well and incubated for 12 h. Cultured cells were pretreated with compound **9** (1, 2, 4 µM/L) for 1 h and incubated with LPS (1 µg/mL) for 12 h. RNA was extracted with Trizol Reagent (Takara Bio Inc., Otsu, Japan) according to the manufacturer's instructions, and cDNA was reverse transcribed from total RNA using a Superscript III system (Takara Bio Inc., Otsu, Japan). PCR amplification was carried out using PikoReal™ (Thermo Fisher Scientific, MA, US) and specific primers. The primer sequences (Wcgene Biotech, Shanghai, China) are shown in Table 3. The optimal conditions for PCR amplification of the cDNA were established by following the manufacturer's instructions. Relative gene expression was calculated using the comparative Ct method (2^{−ΔΔCt}) with glyceraldehyde-3-phosphate dehydrogenase (GAPDH) as an internal control. All experiments were performed in triplicate (n = 3).

Table 3. Primer sequences in this experiment.

Primer		Primer Sequence (5' to 3')
iNOS	Forward	GTCTTTGACGCTCGGAAGTGTAG
	Reversed	TGAAGTCATGTTTGCCGTCCTACT
COX-2	Forward	GATGACTGCCCAACTCCC
	Reversed	AACCCAGGTCCTCGCTTA
TNF- α	Forward	TGGCTGCTGAAAAGACACATGT
	Reversed	CCACCAGACGTTCTGCTGTCTAG
IL-1 β	Forward	AGTTGACGGACCCCAAAAG
	Reversed	AGCTGGATGCTCTCATCAGG
IL-6	Forward	TTCCATCCAGTTGCCTTCTTG
	Reversed	GGGAGTGGTATCCTCTGTGAAGTC
GADPH	Forward	TGTGTCCTCGTGGATCTGA
	Reversed	TTGCTGTTGAAGTCGCAGGAG

4. Conclusions

The 1, 4-naphthoquinone derivatives were reported to show potential anti-inflammatory effect, including reducing 12-O-tetradecanoylphorbol-13-acetate (TPA)-induced acute inflammation in mouse ear [25], suppressing the production of TNF- α induced by LPS in mouse macrophages [25]. Suppressing TNF- α production in serum in vivo mouse model of LPS evoked acute inflammation [25], reducing cotton pellet- and carrageenin-induced paw edema in rat [26], and so on.

In this study, we isolated two new 1, 4-naphthoquinone derivatives, talanaphthoquinone A, B (1, 2), along with 10 known analogues (3–12) from mangrove-derived endophytic fungus *Talaromyces* sp. SK-S009. All the compounds strongly inhibited LPS-induced NO production in RAW264.7 cell line in a dose-dependent manner. The NO production inhibition activities of all the compounds except for compound 2 were more potent than the positive control, indomethacin. Six compounds (1, 7, 9, 10, 11, and 12) showed relatively less cytotoxicity to RAW264.7 cells with SI values varied from 2.1 to 29.6. A primary analysis of the structure–activity relationships was discussed. Furthermore, compound 9 reduced the mRNA levels of iNOS, COX-2, IL-1 β , IL-6, and TNF- α . The results of this study demonstrated that these 1, 4-naphthoquinone derivatives can inhibit LPS-induced inflammation. This is the first report that compound 9 possesses anti-inflammatory activity.

Supplementary Materials: The following are available online, Figures S1–S12: HRESIMS spectrum, 1D- and 2D-NMR spectra of 1 and 2.

Author Contributions: Conceptualization and methodology, H.L. and Z.S.; experiment, H.L., C.Y., C.L., and T.Y.; data curation, H.L.; writing, original draft preparation, H.L. and C.Y.; writing, review and editing, H.L. and Z.S.; funding acquisition, H.L. and Z.S. All authors have read and agreed to the published version of the manuscript.

Funding: This research was funded by PhD researchers of Guangdong Medical University (grant number B2017028), the National Natural Science Foundation of China (grant number 81741162, 21877133, 21472251, 41906033), the Natural Science Foundation of Guangdong Province of China (grant number 2019A1515012084), Guangdong Special Fund for Marine Economic Development (grant number GDME-2018C004), the Key Project of Natural Science Foundation of Guangdong Province (grant number 2016A040403091), and the Special Promotion Program for Guangdong Provincial Ocean and Fishery Technology (grant number A201701C06).

Conflicts of Interest: The authors declare no conflict of interest.

References

1. Heller, R.A.; Schena, M.; Chai, A.; Shalon, D.; Bedilion, T.; Gilmore, J.; Woolley, D.E.; Davis, R.W. Discovery and analysis of inflammatory disease-related genes using cDNA microarrays. *Proc. Natl. Acad. Sci. USA* **1997**, *94*, 2150–2155. [[CrossRef](#)] [[PubMed](#)]
2. Lee, T.S.; Tsai, H.L.; Chau, L.Y. Induction of heme oxygenase-1 expression in murine macrophages is essential for the anti-inflammatory effect of low dose 15-deoxy-delta 12, 14-prostaglandin J2. *J. Biol. Chem.* **2003**, *278*, 19325–19330. [[CrossRef](#)] [[PubMed](#)]
3. Wiesel, P.L.; Foster, C.; Pellacani, A.; Layne, M.D.; Hsieh, C.M.; Huggins, G.S.; Strauss, P.; Yet, S.F.; Perrella, M.A. Thioredoxin facilitates the induction of heme oxygenase-1 in response to inflammatory mediators. *J. Biol. Chem.* **2000**, *275*, 24840–24846. [[CrossRef](#)] [[PubMed](#)]
4. Mayer, A.M.S.; Abimael, D.R.; Tagliatalascasfati, O. Marine pharmacology in 2012–2013: Marine compounds with Antibacterial, antidiabetic, antifungal, anti-inflammatory, antiprotozoal, antituberculosis, and antiviral activities; affecting the immune and nervous systems, and other miscellaneous mechanisms of action. *Mar. Drugs* **2017**, *15*, 2510–2573.
5. Cui, H.; Liu, Y.; Li, J.; Huang, X.; Yan, T.; Cao, W.; Liu, H.; Long, Y.; She, Z. Diaporindenes A–D: Four unusual 2, 3-dihydro-1H-indene analogues with anti-inflammatory activities from the mangrove endophytic fungus *Diaporthe* sp. SYSU-HQ3. *J. Org. Chem.* **2018**, *83*, 11804–11813. [[CrossRef](#)]
6. Liu, H.; Chen, S.; Liu, W.; Liu, Y.; Huang, X.; She, Z. Polyketides with immunosuppressive activities from mangrove endophytic fungus *Penicillium* sp. ZJ-SY2. *Mar. Drugs* **2016**, *14*, 217–223. [[CrossRef](#)]
7. Rosario, N.; Antonio, T. Bioactive compounds produced by strains of *Penicillium* and *Talaromyces* of marine origin. *Mar. Drugs* **2016**, *14*, 37–71.

8. Zhang, L.; Zhang, W.; Liu, J.; Hu, J. C–F bond cleavage by intramolecular SN₂ reaction of alkyl fluorides with O- and N-Nucleophiles. *J. Org. Chem.* **2009**, *74*, 2850–2853. [[CrossRef](#)]
9. Mangasánchez, J.J.; Busto, E.E.; Gotor-Fernández, V.V.; Gotor, V.V. Straightforward synthesis of enantiopure 2, 3-dihydrobenzofurans by a sequential stereoselective biotransformation and chemical intramolecular cyclization. *Org. Lett.* **2010**, *12*, 3498–3501. [[CrossRef](#)]
10. Kimura, Y.; Shimada, A.; Nakajima, H.; Hamasaki, T. Structures of naphthoquinones produced by the fungus, *Fusarium* sp., and their biological activity toward pollen germination. *Agric. Biol. Chem.* **1988**, *52*, 1253–1259. [[CrossRef](#)]
11. Baker, R.A.; Tatum, J.H.; Nemeč, S. Antimicrobial activity of naphthoquinones from *Fusaria*. *Mycopathologia* **1990**, *111*, 9–15. [[CrossRef](#)] [[PubMed](#)]
12. Yang, Z.; Ding, J.; Ding, K.; Chen, D.; Shan, C.; Mei, G. Phomonaphthalenone A: A novel dihydro-naphthalenone with anti-HIV activity from *Phomopsis* sp. HCCB04730. *Phytochem. Lett.* **2013**, *6*, 257–260. [[CrossRef](#)]
13. Medentsev, A.G.; Akimenko, V.K. Mechanism of phytotoxic action of naphthoquinone pigments of the fungus *Fusarium decemcellulare*. *Phytochemistry* **1992**, *31*, 77–79. [[CrossRef](#)]
14. Xia, X.; Liu, X.; Koo, D.C.; Sun, Z.; Shim, S. Chemical constituents of *Fusarium* sp. fungus associated with sea cucumbers. *Chem. Nat. Com.* **2014**, *50*, 1103–1105. [[CrossRef](#)]
15. Moore, R.E.; Singh, H.; Chang, C.W.J.; Scheuer, P.J. Polyhydroxy naphthoquinones: Preparation and hydrolysis of methoxyl derivatives. *Tetrahedron* **1967**, *23*, 3271–3305. [[CrossRef](#)]
16. Xu, Y.; Lu, C.; Zheng, Z. New polyketides isolated from *Botryosphaeria australis* strain ZJ12-1A. *Helv. Chim. Acta* **2011**, *94*, 897–902. [[CrossRef](#)]
17. Poch, G.K.; Gloer, J.B.; Shearer, C.A. New bioactive metabolites from a freshwater isolate of the fungus *Kirschsteiniotelia* sp. *J. Nat. Prod.* **1992**, *55*, 1093–1099. [[CrossRef](#)]
18. Sun, R.; Gao, Y.; Shen, K.; Xu, Y.; Wang, C.; Liu, H. Antimicrobial metabolites from the aquatic fungus *Delitschia corticola*. *Phytochem. Lett.* **2011**, *4*, 101–105. [[CrossRef](#)]
19. Chen, Y.; Liu, Z.; Liu, H.; Pan, Y.; Li, J.; Liu, L.; She, Z. Dichloroisocoumarins with potential anti-inflammatory activity from the mangrove endophytic fungus Ascomycota sp. CYSK-4. *Mar. Drugs* **2018**, *16*, 54. [[CrossRef](#)]
20. Zhao, D.; Shao, C.; Gan, L.; Wang, M.; Wang, C. Chromone derivatives from a sponge-derived strain of the fungus *Corynespora cassiicola*. *J. Nat. Prod.* **2015**, *78*, 286–293. [[CrossRef](#)]
21. Nielsen, K.F.; Smedsgaard, J. Fungal metabolite screening: Database of 474 mycotoxins and fungal metabolites for dereplication by standardised liquid chromatography-UV-mass spectrometry methodology. *J. Chrom. A* **2003**, *1002*, 111–136. [[CrossRef](#)]
22. Arsenault, G.P. Fungal metabolites—III: Quinones from *Fusarium solani* D2 purple and structure of (+)-solaniol. *Tetrahedron* **1968**, *24*, 4745–4749. [[CrossRef](#)]
23. Liu, Y.; Yang, Q.; Xia, G. Polyketides with α -glucosidase inhibitory activity from a mangrove endophytic fungus, *Penicillium* sp. HN29-3B1. *J. Nat. Prod.* **2015**, *78*, 1816–1822. [[CrossRef](#)] [[PubMed](#)]
24. Lee, M.H.; Lee, J.M.; Jun, S.H.; Lee, S.H.; Kim, N.W.; Lee, J.H.; Ko, N.Y.; Mun, S.H.; Kim, B.K.; Lim, B.O. The anti-inflammatory effects of *Pyrolae herba* extract through the inhibition of the expression of inducible nitric oxide synthase (iNOS) and NO production. *J. Ethnopharmacol.* **2007**, *112*, 49–54. [[CrossRef](#)] [[PubMed](#)]
25. Kobayashi, K.; Nishiumi, S.; Nishida, M.; Hirai, M.; Azuma, T.; Yoshida, H.; Mizushima, Y.; Yoshida, M. Effects of quinone derivatives, such as 1, 4-naphthoquinone, on DNA polymerase inhibition and anti-inflammatory action. *Med. Chem.* **2011**, *7*, 37–44. [[CrossRef](#)]
26. Fathy, H.M.; Aboushoer, M.I.; Baraka, A.; Abdel-Kader, M.S.; Omar, A.A. A New Naphthoquinone with Anti-inflammatory Activity from an Egyptian collection of *Echiochilon fruticosum*. *Nat. Prod. Sci.* **2009**, *15*, 22–26.

Sample Availability: Not available.



© 2020 by the authors. Licensee MDPI, Basel, Switzerland. This article is an open access article distributed under the terms and conditions of the Creative Commons Attribution (CC BY) license (<http://creativecommons.org/licenses/by/4.0/>).